Blood vessel closure using photosensitisers engineered for two-photon excitation

Hazel A. Collins[1], Mamta Khurana[2], Eduardo H. Moriyama[2], Adrian Mariampillai[2], Emma Dahlstedt[1], Milan Balaz[1], Marina K. Kuimova[3], Mikhail Drobizhev,[4] Victor X. D. Yang,[2,5] David Phillips[3], Aleksander Rebane,[4] Brian C. Wilson[2]* & Harry L. Anderson[1]*

The spatial control of optical absorption provided by two-photon excitation (TPE) has led to tremendous advances in microscopy[1] and microfabrication[2]. Medical applications of TPE in photodynamic therapy (PDT)[3,4] have often been suggested[5-18], but have been made impractical by the low two-photon cross-sections of photosensitiser drugs (i.e. compounds taken up by living tissues that become toxic on absorption of light). The invention of efficient two-photon activated drugs will allow precise manipulation of treatment volumes in three dimensions, to a level unattainable with current techniques. Here we present a new family of PDT drugs designed for efficient TPE, and use one of them to demonstrate selective closure of blood vessels via TPE-PDT *in vivo*. These conjugated porphyrin dimers have two-photon cross-sections that are more than two orders of magnitude greater than those of clinical photosensitisers[17]. This is the first demonstration of *in vivo* PDT using a photosensitiser engineered for efficient two-photon excitation.

Photodynamic therapy is used to treat diseases characterised by neoplastic growth including various cancers, age-related macular degeneration (AMD) and actinic keratosis[3,4]. Cell death is induced by photoexcitation of a sensitiser, generally via production of singlet oxygen. In the absence of light the photosensitiser is benign, so systemic toxicity is rare and treatment may be repeated without acquired resistance. Two-photon excitation of the photosensitiser should allow greater precision than is attainable by conventional one-photon excitation, as a consequence of the quadratic dependence of TPE on the local light intensity — the amount of TPE is inversely proportional to the fourth power of the distance from the focus. In addition, the longer wavelengths associated with TPE allow treatment deeper into tissue, by minimising absorption from endogenous chromophores.

High instantaneous photon densities are essential for two-photon excitation. Early TPE-PDT studies used nanosecond lasers, but the dominant effect was photothermal damage[5-7]. The advent of commercial femtosecond tuneable Ti:sapphire lasers has greatly facilitated the investigation of TPE-PDT, and the limiting factor has become the availability of suitable photosensitisers. The majority of chromophores possess low two-photon cross-sections, of the order of 1–100 Goeppert-Mayer units (1 GM = 10^{-50} cm^4 s photon^{-1}). For example, the two FDA-approved PDT photosensitisers, verteporfin and Photofrin (cross sections 50 GM and 10 GM respectively)[17], are unlikely to be suitable for TPE-PDT, as the high light intensities needed to achieve a therapeutic effect are close to the thresholds for photothermal or photomechanical damage[18].

Several design strategies for TPE-PDT photosensitisers have been reported recently[11-16], but few of these compounds have yet been studied *in vitro*[15], and, to date, none have progressed to *in vivo* testing. Porphyrin derivatives are often effective PDT agents, as exemplified by verteporfin and Photofrin[4]. Recently it has been found that the two-photon cross-section of a porphyrin can be increased 500-fold by forming a conjugated porphyrin dimer[19-21], and that these dimers have high singlet oxygen yields[20,22]. Here we show that porphyrin dimers can be functionalised with polar substituents to give effective TPE-PDT drugs.

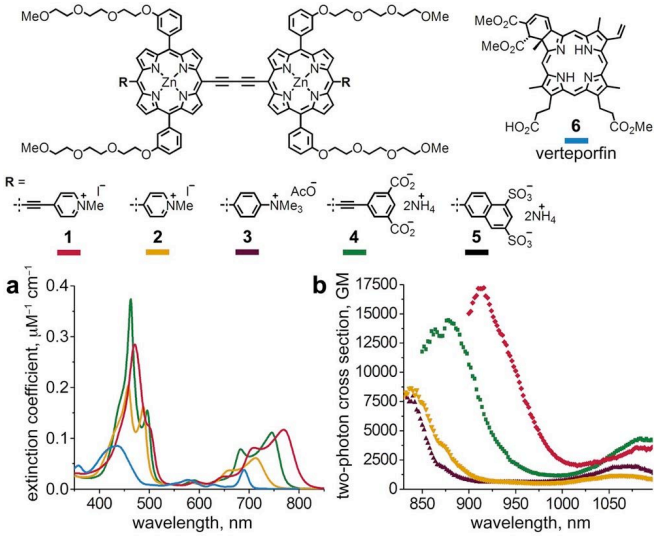

Figure 1 | Structures and absorption spectra of conjugated porphyrin dimers **1**–**5**, and the clinical photosensitiser verteporfin, **6**; (**a**): one-photon absorption spectra of **1**, **2, 4** and **6**, and (**b**) two-photon absorption spectra of **1**–**4**. The spectra of **3** and **5** are almost identical to those of **2**. All spectra were recorded in dimethylformamide (DMF) with 1 % pyridine.

We have tested a family of related anionic and cationic conjugated porphyrin dimers **1**–**5**. The structures of these compounds are shown in Fig. 1, together with their one-photon and two-photon absorption spectra. Polar terminal substituents were added to facilitate delivery to cells. In the case of **1** and **4**, the conjugated electron-accepting aromatic terminals also shift the one-photon and two-photon absorption to longer wavelengths and intensify the two-photon absorption (σ_{max} 17,000 GM at 916 nm for **1**). The singlet oxygen quantum yields, in methanol, are: 0.60, 0.54, 0.70, 0.16 and 0.69 for **1**–**5** respectively, showing that they all have potential as PDT agents. All five compounds are readily internalised by human ovarian adenocarcinoma cells (SK-OV-3), and exhibit punctate fluorescence in the cytoplasm (supplementary information Fig. S2). One-photon PDT experiments (Fig. 2a) show that while the anionic dyes **4** and **5**, have limited PDT activity, the cationic compounds **1**–**3** are comparable to verteporfin **6**. The photodynamic efficiencies of compounds **1**–**3** were investigated in detail, including the effect of incubation time, concentration and light dose (supplementary information Fig. S3). Compound **1** was selected as the most promising candidate because of its high PDT potency, rapid up-take by cells and high two-photon cross-section.

TPE-PDT experiments with dimer **1** were carried out on SK-OV-3 cells, using a Ti:sapphire laser (920 nm, 300 fs, 90 MHz). A confocal microscope was used to irradiate a monolayer of cells and to determine survival by fluorescent staining[17]. The quadratic dependence of the therapeutic effect on the laser intensity (Fig. 2b) confirms that, PDT is achieved via TPE. Under two-photon excitation, porphyrin dimer **1** is substantially more phototoxic than verteporfin and requires only 260 scans to kill 50% of the cells,

[1]Department of Chemistry, Oxford University, Chemistry Research Laboratory, 12 Mansfield Road, Oxford OX1 3TA, UK. [2]Department of Medical Biophysics, Ontario Cancer Institute, University of Toronto, Toronto M5G 2M9, Canada. [3]Chemistry Department, Imperial College London, Exhibition Road, London SW7 2AZ, UK. [4]Department of Physics, Montana State University, Bozeman, Montana 5917-384, USA. [5]Department of Physics, Ryerson University, Toronto M5B 2K3, Canada.

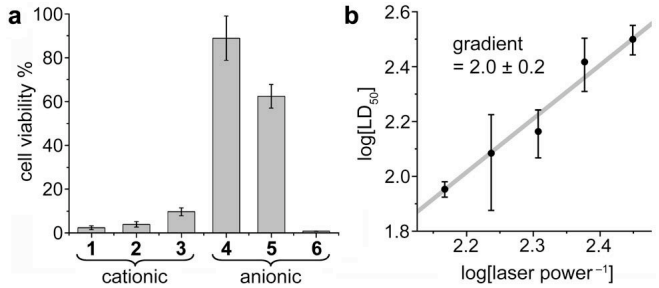

Figure 2 | *In vitro* photodynamic therapy. (**a**) One-photon photodynamic efficiencies of porphyrin dimers **1**–**5**, compared to verteporfin, **6**. Human ovarian adenocarcinoma cells (SK-OV-3) were incubated with 10 μM of each photosensitiser for 6 h and irradiated with 657 nm light, 3.2 mW, 20 min. Cell viability was determined using a MTT assay[23]. Neither light nor drugs were individually toxic to the cells at these doses; average cell viability 97% ± 12 and 101% ± 12 respectively (error bars: 1 s.d.). (**b**) Two-photon photodynamic efficiency of **1** as a function of laser power, determined as in Khurana *et al.*[17] (error bars: 1 s.e.). The SK-OV-3 cells were incubated for 18 h, with 10 μM of **1** and irradiated with 920 nm, 300 fs, 90 MHz light. The light dose (number of scans) required to kill 50% of the cells (LD_{50}), was determined using 3.6, 4.2, 4.9, 5.8 and 6.8 mW powers (supplementary information Fig. S4), and $\log[LD_{50}]$ is plotted against $\log[\text{laser power}^{-1}]$. The gradient of the linear fit to these points is 2.0 ± 0.2, confirming two-photon activation.

whereas 430 scans are required with verteporfin (4.2 mW laser power, supplementary information Fig. S5).

TPE-PDT holds particular promise for the targeted closure of blood vessels associated with neoplastic diseases, especially for the treatment of complex organs such as the eye or brain, where high

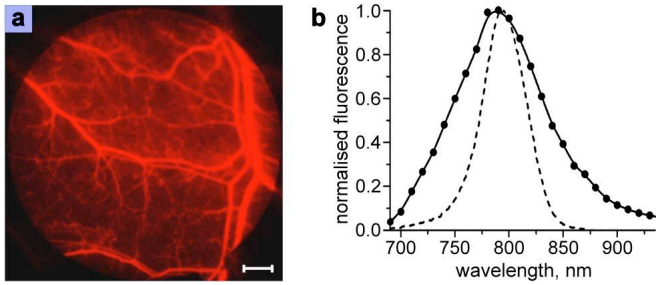

Figure 3 | Fluorescence from photosensitiser 1 *in vivo*. (**a**) Wide-field *in vivo* fluorescence image (λ_{ex} 445–490 nm, λ_{em} 690–940 nm in 10 nm bands, Maestro, CRi) of **1** through the window chamber, 1 h post tail vein injection, 10 mg kg^{-1} (scale bar: 1 mm). Photosensitiser **1** was prepared from a 10 mM stock in DMSO diluted with 5 % dextrose (Baxter). Autofluorescence was subtracted from the images by deconvolution. (**b**) The resulting emission spectrum of **1** in the blood (—), and the corresponding emission spectrum in DMF with 1% pyridine (- - -).

spatial selectivity is crucial[10,18]. We sought to test the selective closure of blood vessels *in vivo* with photosensitiser **1**, using the dorsal skinfold window chamber model for non-invasive visualisation of blood vessels[24]. The inner skin layer of a male athymic nude mouse (NCRNU-M, Taconic) was removed from a 10 mm diameter region and a titanium saddle was sutured in place to hold the skin flap vertically away from the body. The exposed facial plane and associated vasculature were protected with a glass coverslip (145 ± 15 μm thick). Surgery and treatment were carried out under continuous ketamine-xylazene aesthesia. Porphyrin dimer **1** was administered via the tail vein in 5 % dextrose solution and its fluorescence was imaged through the window (Fig. 3a). The

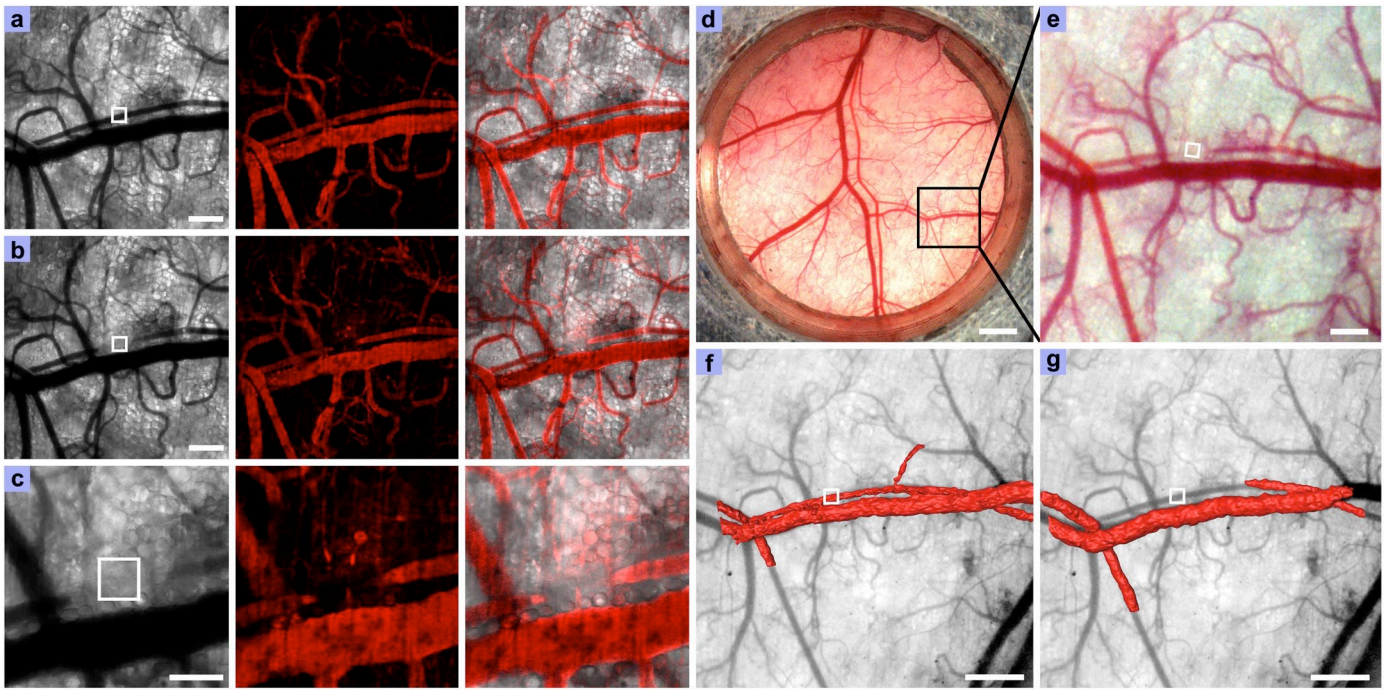

Figure 4 | *In vivo* two-photon blood vessel closure with photosensitiser 1. Mice bearing dorsal window chambers were administered 10 mg kg^{-1} of **1** diluted from a 10 mM stock in DMSO. A selected artery was targeted with 920 nm light (< 3 mW) guided by the striations caused by blood flow visible in the transmission image (supplementary information Fig. S7). An 83 × 83 × 40 μm volume was irradiated 4 times (39 mW) as a stack of 5 planes, 10 μm apart; each plane consists of 512 × 512 pixels; dwell time: 0.8 μs per pixel. **a**, Pre-treatment confocal (5×, 0.25 numerical aperture) transmission (left, λ_{ex} 543 nm), TRITC-dextran fluorescence (middle, λ_{ex} 543 nm, λ_{em} 565–615 nm) and superimposed (right) images (scale bar 200 μm). **b**, Images immediately after TPE-PDT with **1** (scale bar 200 μm) and **c**, expanded image of irradiated area (scale bar 100 μm). **d**, Pre-treatment stereomicroscope image of the entire dorsal window chamber (scale bar 1 mm) and **e**, post-treatment image (scale bar 200 μm). 3D-rendered images of blood flow produced by Doppler OCT imaging **f**, pre- and **g**, post-treatment (scale bar 400 μm), overlaid on pre-treatment stereomicroscope image. The blood flow in the targeted artery is from left to right. The white boxes indicate the irradiated region.

emission spectrum of **1** in the blood stream matches that recorded in DMF (Fig. 3b), although the *in vivo* spectrum is slightly broader.

To demonstrate closure of blood vessels using two-photon PDT, we selected arteries with a diameter of 40 ± 5 μm. Laser light (920 nm, 300 fs, 90 MHz, 39 mW) was focussed by a 5×, 0.25 numerical aperture air lens. With this objective, the 1/*e* radius of the two-photon excitation volume was calculated to be 0.83 μm laterally and 11 μm axially[1]. A section of the artery was irradiated as a series of five 83 × 83 μm images, each 10 μm apart through the depth of the vessel. As is used clinically with verteporfin-PDT treatment of AMD, the light dose was applied a short time (15 min) after injection of the photosensitiser[25]. An additional fluorescent marker, tetramethylrhodamine (TRITC) labelled dextran, was also used to facilitate confocal imaging of blood vessels. Mice treated with 10 mg kg^{-1} of photosensitiser **1** and 15 mg kg^{-1} of TRITC-dextran showed vessel thinning during irradiation and the blood flow ceased after 7–12 min continuous raster-scanning; the entire light dose was delivered over 15 min. Immediately after irradiation the artery appeared thinner, and a segment of the vessel approximately 100 μm either side of the centre of the irradiated region was no longer visible in the transmission image (probably due to the exclusion of haemoglobin), Fig. 4a–c. Although the occluded length of the artery is longer than the irradiated region, surrounding blood vessels appear unaffected. Loss of blood vessel function was confirmed by injection of 5 mg kg^{-1} fluorescein labelled dextran after treatment. Fluorescence from this second blood tracer was seen in the surrounding vessels and in the unexposed length of the artery, though the irradiated section remained dark (supplementary information Fig. S8).

Blood vessel closure by injection of 10 mg kg^{-1} of **1** and irradiation with light for 15 min was reproducible, with all 3 animals in the treatment group exhibiting the same outcome (supplementary information Fig. S9). Two additional control groups of three similar sized arteries were exposed to the same light dose. The first group of animals were administered only the TRITC-dextran blood contrast agent (15 mg kg^{-1}). Transmission and fluorescence microscopy confirmed that there were no visible effects to the vessels, proving that the artery closure observed with **1** is not thermal in origin. The remaining group of three animals were injected with the same amount of active photosensitiser (3.25 mg kg^{-1} verteporfin **6**, formulated as 180 mg kg^{-1} of Visudyne®). Significantly, vessel closure could not be induced using prolonged exposure to 920 nm light and verteporfin (supplementary information Fig. S10).

For one animal in each treatment group (10 mg kg^{-1} of 1, 3.25 mg kg^{-1} verteporfin, control) the blood flow pre- and post-irradiation was monitored by optical coherence tomography (OCT, Fig. 4f–g)[26]. A swept laser source scanning 1260–1360 nm was used to map the tissue structure at near histological resolution (~10 μm) by spectral reflectometry. In addition the Doppler frequency shift[27,28] induced by moving red blood cells was used to measure the flow velocity as low as 100 μm s^{-1}. For animals administered TRITC-dextran with or without verteporfin the blood flow remained unaltered by the light dose (supplementary information Figs. 10, 11). In contrast, the flow reduced from 7000 μm s^{-1} to <100 μm s^{-1} in the treated region of the animal administered **1** (supplementary information Table S1). Three-dimensional images showing the surfaces of the blood vessels were constructed for each animal from 1000 transverse scans. The occlusion of the blood vessel by two-photon PDT is clearly evident in the rendered image, Fig. 4f–g.

In summary, we have synthesised a new family of PDT sensitisers derived from porphyrin-based molecular wires with high two-photon cross-sections. The *in vitro* two-photon efficacy of compound **1** offers a significant improvement over the commercial photosensitiser verteporfin **6**. This is the first time a photosensitiser designed specifically to have a high two-photon cross-section has been shown to be effective *in vivo*, and the first demonstration of TPE-PDT in a living mammal. Although the energy density required for two-photon vessel-closure with near-IR light is higher than would be required for one-photon closure with visible light, there is no detectable photothermal damage because the tissue is essentially transparent at the illumination wavelength (920 nm). This study highlights the feasibility of two-photon photodynamic therapy as a new strategy for targeted occlusion of blood vessels.

METHODS

Two-photon absorption spectra were measured by means of fluorescence intensity (justified by Vavilov–Kasha's rule). For two-photon excitation, we used linearly polarized light from a tuneable femtosecond optical parametric amplifier (TOPAS, Quantronix) and recorded the fluorescence emission of freshly prepared samples (ca. 1 μM solution in a 1 cm cuvette) in 90° geometry as a function of excitation wavelength with an imaging spectrometer (Triax 550, Jobin-Ivon). Spectra were corrected for the wavelength dependence of photon flux, pulse duration, and beam spatial profile. These spectra were scaled to the cross-section (σ), measured at a selected wavelength. For σ measurement, we compared the intensities of one- and two-photon excited fluorescence under the same conditions of registration and similar excitation geometry.[29]

Singlet oxygen quantum yields were determined with reference to chlorophyll *a* in methanol (0.77)[30] by excitation with 450 nm, 9 ns, 10 Hz, 0.05–3 mW light from a pulsed dye laser (Lambda Physik with coumarin 120 in methanol) pumped by a frequency doubled Nd:YAG laser (Continuum Surelite I-10). The singlet oxygen luminescence at 1270 nm was detected perpendicular to the excitation beam using a cooled photodiode (E0817-P North Coast) and the signal was averaged and recorded using a digital oscilloscope (Tektronics TDS 3012).

Confocal microscopy. A laser scanning microscope (LSM 510 Meta NLO, Zeiss) equipped with argon ion (488 nm), He-Ne (543 nm) and Ti:sapphire lasers (Chameleon, Coherent, tuneable from 730 nm to 960 nm, 300 fs, 90 MHz) was used for confocal imaging and two-photon irradiation. *In vitro* studies used a 40×, (NA 1.2, water immersion) objective and the cells were maintained at 37 °C. A 5× (NA 0.25) was used for *in vivo* work, and the mice were maintained normothermic at 30 °C.

***In vitro* imaging.** SK-OV-3 cells (ECACC) were grown in phenol red free DMEM (Gibco) supplemented with 2 mM *L*-glutamine, 100 U mL^{-1} penicillin (Sigma), 100 μg mL^{-1} streptomycin (Sigma) and 10 % fetal bovine serum (Sigma). The cells were maintained at 37 °C in a humidified 5 % CO_2 atmosphere. The cells were detached from the flasks with a solution of 0.05 % *w/v* trypsin (Gibco) and seeded, 2.4×10^5 cells in 400 μL of medium, in untreated 8-well coverglass chambers (Lab-Tek™ chambered coverglass, Nunc) and allowed to grow to confluence over 3 days. The localisation of **1** was determined after 4 h incubation with 10 μM diluted in culture medium from a 1 mM stock in DMSO (λ_{ex} 458 nm, λ_{em} 650–710 nm).

***In vitro* phototoxicity**. SK-OV-3 cells were seeded in flat 96-well plates (Nunc), 1250 cells per well in 100 μL of media and irradiated 26 h later. At the required time before the light dose, the media on the cells was replaced with the photosensitiser solution. The plates were shielded from light during and after incubation. The wells requiring light exposure were irradiated with 657 nm LEDs (3.2 mW, Dotlight GbR, Germany), then washed (3 × 100 μL media) and incubated in 100 μL of media for 42 h. After this time the cell viability was determined using a proliferation assay (CellTiter 96® Aqueous, Promega). An average background absorbance reading of the media was recorded and subtracted from the average absorbance of each replicate group. Each experiment consisted of at least 5 replicates, and every experiment was repeated at least three times.

Mice. All *in vivo* work was performed with ca. 20 g nude male NCRNU-M (Taconic) mice, anesthetised with 80 mg kg^{-1} ketamine and 13 mg kg^{-1} xylazine i.p., kept anesthetised with 30 min injections of quarter this dose, in accordance with approved protocol 1311.4 of the University Health Network, Toronto. Dorsal window chambers were installed as described previously[24].

Stereomicroscopy. Pre- and post-irradiation the vasculature of the window chamber was imaged using a stereomicroscope (MZ FLIII, Leica). 1× magnification, white light mode

Optical coherence tomography was performed using a 24 kHz swept source OCT system (OCM1300SS, Thorlabs) with an isotropic spatial resolution of 10 μm. 3D image stacks were acquired before and after two-photon light exposure in a 1 mm^3 cubic volume of interest. The irradiated regions were selected using the real-time colour Doppler mode to identify blood vessels. Both structural and Doppler images were collected and processed for peak blood flow velocity estimation and 3D rendering.

Doppler background noise was first minimized using a histogram rejection algorithm after which the peak blood flow velocity estimates were made[28]. For 3D visualizations a consecutive series of segmented blood vessels images was used to reconstruct the vessel surfaces, which were subsequently rendered using image processing software (Amira 4.1.1, Mercury Computer Systems).

Two-photon irradiation of arteries: Before irradiation mice bearing window chambers were injected with 15 mg kg^{-1} of 2,000,000 MW dextran labelled with tetramethyl rhodamine (Molecular Probes) and a maximum of two arteries with a diameter of 40 ± 5 μm were selected by confocal fluorescence microscopy (λ_{ex} 543 nm, λ_{em} 565–615 nm). For the treatment groups mice were administered by tail vein injection either 10 mg kg^{-1} of **1** diluted from a 10 mM stock in DMSO or 3.25 mg kg^{-1} of verteporfin with TRITC-dextran. The verteporfin was administered as the clinical formulation Visudyne® (QLT Inc.): 180 mg kg^{-1} of Visudyne® was used as it contains 3.25 mg kg^{-1} of verteporfin, an equivalent photosensitiser dose as used with **1**, scaled to account for their differing molecular weights. The artery was focused using 920 nm light (< 3 mW) and an 83 × 83 μm region was irradiated (39 mW) as a vertical stack of 5 images, each 10 μm apart. A minimum of 1 h post irradiation 5 mg kg^{-1} of 464,000 MW dextran labelled with fluorescein (Sigma) was injected in 100 μL of 5 % dextrose and imaged 15 min later (λ_{ex} 488 nm, λ_{em} long pass 505 nm).

1. Zipfel, W. R., Williams, R. M., & Webb, W. W. Nonlinear magic: multiphoton microscopy in the biosciences. *Nature Biotech*. 21, 1369–1377 (2003).
2. Cumpston, B. H. *et al.* Two-photon polymerisation initiators for three-dimensional optical data storage and microfabrication. *Nature* 398, 51–54 (1999).
3. Castano, A. P., Mroz, P. & Hamblin, M. R. Photodynamic therapy and anti-tumour immunity. *Nature Rev. Cancer* 6, 535–545 (2006).
4. Macdonald, I. J. & Dougherty, T. J. Basic principles of photodynamic therapy, *J. Porphyrins Phthalocyanines* 5, 105–129 (2001).
5. Marchesini, R. *et al.* A study on the possible involvement of nonlinear mechanism of light absorption by HpD with Nd:YAG laser. *Lasers Surg. Med.* 6, 323–327 (1986).
6. Patrice, T. M. *et al.* Neodymium-yttrium aluminium garnet laser destruction of nonsensitized and hematoporphyrin derivative-sensitised tumors. *Cancer Res*. 43, 2876–2879 (1983).
7. Lenz, P. *In vivo* excitation of photosensitizers by infrared light. *Photochem. Photobiol*. 62, 333–338 (1995).
8. Fisher, W. G., Partridge, W. P., Dees, C. & Wachter, E. A. Simultaneous two-photon activation of type-I photodynamic therapy agents. *Photochem. Photobiol.* 66, 141–155 (1997).
9. Bhawalkar, J. D., Kumar, N. D., Zhao, C. F. & Prasad, P. N. Two-photon photodynamic therapy, *Lasers Surg. Med.* 15, 201–204 (1997).
10. Samkoe, K. S. & Cramb, D. T. Application of an *ex ovo* chicken choriallantoic membrane model for two-photon excitation photodynamic therapy of age-related macular degeneration. *J. Biomed. Optics* 8, 410–417 (2003).
11. Karotki, A., Kruk, M., Drobizhev, M., Rebane, A., Nickel, E. & Spangler, C. W. Efficient singlet oxygen generation upon two-photon excitation of a new porphyrin with enhanced nonlinear absorption, *IEEE J. Select. Topics Quantum Electon.* 7, 971–975 (2001).
12. Spangler, C. W., Starkey, J. R., Rebane, A., Meng, F., Gong, A. & Drobizhev, M. Synthesis, characterisation and preclinical studies of two-photon-activated targeted PDT therapeutic triads, *Proc. SPIE*. 6139, 61390X-1–10 (2006).
13. Oar, M. A. *et al.* Light-harvesting chromophores with metalated porphyrin cores for tuned photosensitization of singlet oxygen via two-photon excited FRET. *Chem. Mater.* 18, 3682–3692 (2006).
14. Dy, J. T., Ogawa, K., Satake, A., Ishizumi, A. & Kobuke, Y. Water-soluble self-assembled butadiyne-bridged bisporphyrin: a potential two-photon-absorbing photosensitizer for photodynamic therapy. *Chem. Eur. J.* 13, 3491–3500 (2007).
15. Kim, S., Ohulchanskyy, T. Y., Pudavar, H. E., Pandey, R. K. & Prasad, P. N. Organically modified silica nanoparticles co-encapsulating photosensitizing drug and aggregation-enhanced two-photon absorbing fluorescent dye aggregates for two-photon photodynamic therapy. *J. Am. Chem. Soc*. 129, 2669–2675 (2007).
16. Arnbjerg, J. *et al.* Two-photon absorption in tetraphenylporphycenes: are porphycenes better candidates than porphyrins for providing optimal optical properties for two-photon photodynamic therapy? *J. Am. Chem. Soc.* 129, 5188–5199 (2007).
17. Khurana, M. *et al.* Quantitative in vitro demonstration of two-photon photodynamic therapy using Photofrin® and Visudyne®. *Photochem. Photobiol.* 83, 1441–1448 (2007).
18. Samkoe, K. S., Clancy, A. A., Karotki, A., Wilson, B. C. & Cramb, D. T. Complete blood vessel occlusion in chick chorioallantoic membrane using two-photon excitation photodynamic therapy: implications for treatment of wet age-related macular degeneration. *J. Biomed. Opt*. 12, 034025-1–14 (2007).
19. Drobizhev, M. *et al.* Understanding strong two-photon absorption in π-conjugated porphyrin dimers via double-resonance enhancement in a three-level model. *J. Am. Chem. Soc.* 126, 15352–15353 (2004).
20. Drobizhev, M. *et al.* Extremely strong near-IR two-photon absorption in conjugated porphyrin dimers: quantitative description with three essential states model. *J. Phys. Chem. B.* 109, 7223–7236 (2005).
21. Ogawa, K. *et al.* Strong two-photon absorption of self-assembled butadiyne-linked bisporphyrin. *J. Am. Chem. Soc.* 125, 13356–13357 (2003).
22. Kuimova, M. K. *et al.* Determination of the triplet state energies of a series of conjugated porphyrin oligomers. *Photochem. Photobiol. Sci.* 6, 675–682 (2007).
23. Cory, A. H., Owen, T. C., Barltrop, J. A. & Cory, J. G. Use of an aqueous soluble tetrazolium/formazan assay for cell growth assays in culture. *Cancer Commun*. 3, 207–212 (1991).
24. Algire, G. H. & Legallais, F. Y., Recent developments in the transparent-chamber technique as adapted to the mouse. *J. Natl. Cancer Inst.* 10, 225–253 (1949).
25. Photodynamic therapy of subfoveal choroidal neovascularization in age-related macular degeneration with verteporfin: one-year results of 2 randomized clinical trials – TAP report 1. *Arch. Ophthalmol*. 117, 1329–1345 (1999).
26. Huang, D. *et al*. Optical coherence tomography. *Science* 22, 1178–1181 (1991).
27. Mariampillai, A. *et al.* Optical cardiogram gated 2D Doppler flow imaging at 1000 fps and 4D imaging at 36 fps on a swept source OCT system. *Opt. Express* 15, 1627–38, (2007).
28. Yang, V. X. D. *et al*. Improved phase-resolved optical Doppler tomography using the Kasai velocity estimator and histogram segmentation. *Opt. Commun.* 208, 209–214 (2002).
29. Karotki, A. *et al.* Enhancement of two-photon absorption in tetrapyrrolic compounds. *J. Opt. Soc. Am. B* 20, 321–332 (2003).
30. Wilkinson, F., Helman, W. P. & Ross, A. B. Rate constants for the decay and reactions of the lowest electronically excited singlet-state of molecular-oxygen in solution — an expanded and revised compilation, *Journal of Physical and Chemical Reference Data*. 24, 663–1021 (1995).

Supplementary information is linked to the online version of the paper at www.nature.com/nature.

Acknowledgements. We thank M. K. Akens, T. D. McKee and K. Patel for assistance with tail vein injections, J. Jonkman and G. Netchev for microscopy assistance, the EPSRC Mass Spectrometry Service (Swansea) for mass spectra and Thorlabs Inc. for support with OCT imaging. This work was supported by grants from EPSRC (to H.L.A. and D.P.), the Canadian Institute for Photonic Innovations (to B.C.W.) and the European Commission (Marie Curie Fellowship to M.B., MEIT-CT-2006-041522).

Author Contributions. H.A.C., E.D. and M.B. synthesised the porphyrin dimers. H.A.C. and E.D. screened the compounds *in vitro*. M.D. and A.R. measured the two-photon absorption spectra. M.K.K. measured singlet oxygen yields. E.H.M. and M.K. implanted the window chambers. A.M. imaged vessels by OCT, M.K. by stereomicroscopy and H.A.C. by hyperspectral and laser scanning techniques. All authors discussed the results and contributed to the manuscript.

Author information. Reprints and permissions information is available at npg/nature.com/reprintsandpermissions. The authors declare no competing financial interests. Correspondence and requests for materials should be addressed to H.L.A. (harry.anderson@chem.ox.ac.uk) or B.C.W. (wilson@uhnres.utoronto.ca).